A Production Simulation Tool for Systems With Integrated Wind Energy Resources

Nicolas Maisonneuve and George Gross, *Fellow, IEEE*

***Abstract*—The rapid increase in wind power capacity over the past decade has resulted from the adoption of policies that encourage the wider use of renewable energy sources in order to reduce CO_2 and the dramatic cost reductions due to technology advancements. The high variability in wind speeds poses major difficulties in power system planning and operations, leading to an acute need for practical planning and operations tools to study the effects of the integration of wind resources into the grid. This paper addresses the need in the planning domain through the development of a computationally efficient probabilistic production simulation approach with the capability to quantify the variable effects of systems for varying levels of wind penetration with the uncertainty in the variability/intermittency effects of wind generation at multiple sites together with the other sources of uncertainty explicitly represented. The simulation approach is based on the identification of the prevailing wind regimes in the regions where wind resources are located and the judicious application of conditional probability concepts in incorporating the wind regime representation. The regimes-based approach described in the paper effectively captures both the seasonal and the diurnal variations of renewable resources and their correlation with the load seasonal and diurnal changes. Additionally, the proposed approach explicitly quantifies the impacts of wind on the additional reserve requirements on the controllable resources. The paper illustrates the effectiveness of the approach by its application to large-scale test systems using historical data.**

***Index Terms*—Intermittency effects, probabilistic production simulation, renewable energy, wind integration, wind regimes, wind uncertainty and variability.**

I. Introduction

THE growing concern over the impacts of global warming has resulted in legislation in numerous jurisdictions to curb greenhouse gas emissions and to established initiatives to require the use of renewable resources for electricity supply. For instance, more than half the U.S. states have set ambitious goals through their Renewable Portfolio Standards (*RPS*) specifying the percentage of the electric energy that needs to be served by renewable resources by specific target dates [1]. Wind-based electricity production, which incurs no fuel costs and emits no pollution, has become the prominent leader in the drive to clean energy. The extensive construction of wind farms in the U.S. and other parts of the world has made wind the fastest growing source of new electricity capacity. In Europe, Denmark has become the leader of the integration of wind resources into the grid, with 24% of its electric consumption supplied by wind energy [2]. Some of the other nations with a significant portion of their electric demand served by wind include Spain (14.4%), Portugal (14%), Ireland (10.1%), or Germany (9.4%) [2]. Unfortunately, wind energy also poses major challenges to its effective integration into the grid. An inherent characteristic of wind speed is its high variability, impacting markedly the times and the quantities of wind energy production. In addition, the randomness of wind speed and the lack of controllability of wind energy pose major challenges to the reliable and economic integration of wind generation.

The wind energy production is used to serve the demand by displacing some of the expensive and polluting thermal generation. Since system operators cannot control the outputs of wind resources, the wind energy is used whenever available with the explicit aim of avoiding wind energy "spill"—unnecessarily shutting down the wind resource even though the wind speed is in the allowable range to produce electricity. The extent to which the wind energy and the load are correlated is, consequently, an important consideration in the effective utilization of wind. Clearly, the benefits obtained with the integration of wind resources are higher if the periods with high wind output coincide with those with the high loads. The assessment of the temporal characteristics of the loads and the wind generation and their correlation are required. Unlike the variability in the wind speeds, the loads follow well-defined diurnal and weekly patterns with loads being higher in the week days than on the weekend and experiencing their peaks during the work day and lower values during the nights. In Fig. 1, we provide a plot of the hourly load shape of *MISO*, a regional transmission organization, to illustrate the hourly demands for a winter week. A salient characteristic is the cyclic nature of the daily load each workday. For the same week, we show the wind power output of the MISO system, clearly indicating that the periods with high (low) wind output do not coincide with the high (low) loads. Such uncorrelated behavior complicates the integration of wind resources into the grid and is strongly seasonally dependent. Most U.S. utility systems are summer peaking with the load experiencing its highest values of the year due to the extensive air conditioning usage. This phenomenon produces strong misalignment between the loads and the wind outputs due to the reduction in wind outputs during the summer period, further complicating wind integration into the grid. The impacts of wind integration on reliability are evident from the February 26, 2008, ERCOT event, when the operators had to shed some responsive load as the lack of supply was becoming too pronounced, resulting in

Manuscript received August 30, 2010; revised February 28, 2011; accepted April 06, 2011. Date of publication June 02, 2011; date of current version October 21, 2011. This work was supported by NSF Award # 0925754, GCEP (Stanford University), PSERC, and the Grainger Foundation. Paper no. TPWRS-00676-2010.

The authors are with the Electrical and Computer Engineering Department, University of Illinois at Urbana-Champaign, Urbana, IL 61801 USA (e-mail: nmaison2@illinois.edu; gross@illinois.edu).

Color versions of one or more of the figures in this paper are available online at http://ieeexplore.ieee.org.

Digital Object Identifier 10.1109/TPWRS.2011.2143437

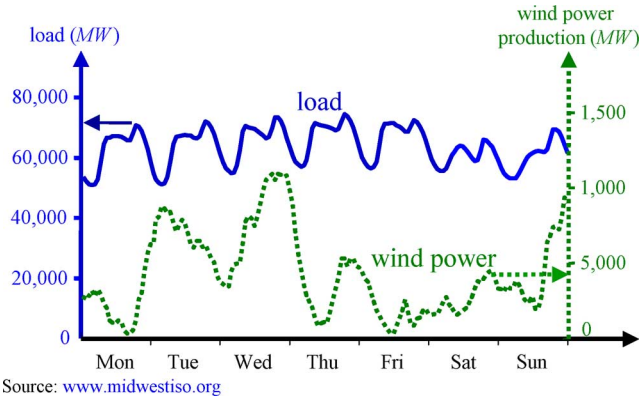

Fig. 1. Chronological *MISO* hourly loads and wind power outputs for the January 7–13, 2006 period.

a frequency drop that threatened the system stability [3]. The ERCOT reliability event illustrates the criticality to appropriately manage wind generation variability and the need to compensate for the lack of predictability [4]. Without large-scale storage devices, operators manage the uncertainty effects by increasing the levels of the system operating reserves [5], resulting in increased system production costs [6]. Consequently, there is an acute need for appropriate tools to study the effects of the integration of wind resources into the grid over longer-term periods. Such tools need to be able to capture the time-dependent wind patterns and their correlated behavior with the system load so that reliability events, such as the one on February 2008 in ERCOT, are explicitly represented. More precisely, the complications arising in the ERCOT event of the suddenly decreased wind power production while the high load levels persisted need to be effectively captured by such tools so as to quantify the variable effects—economics, environmental, and reliability.

While many wind integration studies employ chronological production simulation to assess the wind integration economic and environmental benefits [6], [7], little work has been done on the representation of the effects of the additional uncertainty due to wind resource integration, particularly over longer-term periods. A major challenge is the incorporation of such effects in the probabilistic production simulation framework [8]. In this paper, we describe the construction and testing of a practical approach to quantify the variable effects of systems with integrated wind resources over longer-term periods. We extend the probabilistic production simulation approach so that it can capture the additional sources of uncertainty associated with wind generation and can represent the impacts of the wind resource integration on the power system production costs, CO_2 emissions, and reliability. The extension uses the wind speed regimes model that we developed for a multi-site wind farm power system. The model explicitly represents the variability and the uncertainty in the wind speed and wind power production and is constructed making detailed use of statistical clustering algorithms. We develop a systematic approach to identify classes of days with similar wind patterns at the multiple sites and we probabilistically represent the wind speed for each class. The incorporation of the wind regime model into the probabilistic production simulation framework is accomplished by effective application of conditional probability concepts to the probabilistic representation of the load random variable. In this way, the proposed methodology can explicitly represent the salient, time-varying patterns of the wind generation. Such an approach differs from the existing techniques that represent the wind power production random variable by a multi-state probability distribution [9].

We construct the extended production costing methodology and simulate systems with integrated wind resources, explicitly representing uncertainty in the wind resources in addition to that of other resources and loads. The primary application of the extended production simulation tool is to quantify the impacts of the integration of wind resources into the system on the variable effects over longer-term periods. We illustrate the application of the tool using the extensive studies we performed under a wide range of conditions and on systems in different geographic regions. The studies we discuss provide a realistic assessment of the impacts of the wind energy variability and intermittency on the systems' expected production costs, CO_2 emissions, and reliability metrics.

The paper has additional sections. We focus on the wind regime modeling in Section II and discuss the construction of the extended probabilistic simulation in Section III. In Section IV, we present representative results from the extensive set of simulations performed with the proposed methodology. We summarize the paper and provide directions for future work in Section V.

II. Wind Resource Modeling

The quantification of the longer-term impacts of wind resource integration into the grid requires a wind generation model with the appropriate level of detail for representing the uncertainty in the wind speed and its impacts on the wind power output. We present in this section such a model to explicitly represent the variability and intermittency characteristics of the wind resources for integration into the probabilistic simulation framework [8]. The intended application is to planning activities and so the level of detail is commensurate with the requirements of such a planning tool.

The diurnal wind-farm power production pattern directly impacts the scheduling of the controllable resources. Indeed, if the wind energy production is high during the high-load periods, the wind resources can displace one or more peaking—and, typically, expensive—controllable units. On the other hand, if the wind energy production is significant during the low-load periods, the system operators need to lower the output of the base loaded—and not-so-flexible—units. As the shape of the daily wind power production depends directly on the diurnal wind speed pattern, the wind speed model must reflect this characteristic. Since multiple daily patterns may occur throughout the period under consideration, we first identify the various wind speed regimes by grouping into distinct classes the days whose wind speed patterns have similar "shapes", with as many classes as desired to meet some specified tolerance.

Let D be the number of days in the study period for wind speed data collection, e.g., $D = 365$ for a one-year data set. We partition each day into H non-overlapping subperiods to analyze the wind speed data. We assume that the wind speed is constant over each subperiod. The subperiod duration is the smallest indecomposable unit of time and no phenomena with shorter durations may be represented in the model. Let $v_{s,d}^{(h)}$ denote the wind speed at site s on the day d for the subperiod h. We construct $\underline{v}_{s,d} \triangleq [v_{s,d}^{(1)} \cdots v_{s,d}^{(H)}]^T$, the wind speed vector at

the site s on day d. We use $\underset{\sim}{v}_{s,d}$ to construct the super vector $\underset{\sim}{v}_d \triangleq [\underset{\sim}{v}_{1,d}^T \cdots \underset{\sim}{v}_{S,d}^T]^T$ of the day d wind speed vectors. Our objective is to construct k classes $\mathscr{R}_r$, $r = 1, \ldots, k$, with each class grouping a set of *similar* days of wind speed $\underset{\sim}{v}_d$. Various schemes are used to perform such clustering operations [10], [11]. For the identification of wind regimes, the *hierarchical clustering and the k-means algorithms* are particularly useful. Once we construct the k sets of similar days of wind speed data, we define and characterize the wind speed regimes. Conceptually, we view each class $\mathscr{R}_r$, $r = 1, \ldots, k$, to consist of the realizations in the data set of the random variables (*r.v.*s) $\underset{\sim}{V}_{s,r}^{(h)}$ of the wind speed at site s in the subperiod h. We can use the samples in the set $\mathscr{R}_r$ to estimate the mean value $m_{s,r}^{(h)}$ or the higher moments of each *r.v.* $\underset{\sim}{V}_{s,r}^{(h)}$, as well as their joint probability *c.d.f.* (cumulative distribution function) and *p.d.f.* (probability density function). The probability α_r associated with each class $\mathscr{R}_r$ is approximated by the ratio $\hat{\alpha}_r = |\mathscr{R}_r|/D$ since the set $\mathscr{R}_r$ contains $|\mathscr{R}_r|$ days of the data set. We refer to the pair of estimates of the joint *c.d.f.* of the wind speed *r.v.*s and $\hat{\alpha}_r$ as a regime denoted by $\boldsymbol{R}_r$. The wind speed regime model uses the partitioning of each day into H subperiods. For concreteness, we adopt an hourly resolution[1] with $H = 24$.

We use the regimes for the modeling of the wind power output from a turbine and to construct the model of the wind power output of a wind farm locates at site s. We start with focusing our analysis on the behavior of a stand-alone wind turbine typically characterized by the so-called power curve $g(\cdot)$, with $p_s = g(v_s)$. Here, v_s is the wind speed driving the turbine and p_s is the wind power output of the wind turbine. The shape of the power curve depends on the turbine technology and its operation. Typically, we can represent the output as a piece-wise continuous function [12].

We next discuss the steps to extend the modeling of a stand-alone wind turbine so as to represent the energy output of a wind farm at site s. Let $\mathscr{C}_s = \{c_s : c_s = 1, \ldots, C_s\}$ be the index set of the wind turbine technology types implemented at site s with n_{c_s} being the number of wind turbines of type c_s. A wind turbine of technology type c_s produces a wind power p_{c_s} when experiencing wind speed v_s and is, therefore, described by the power curve $g_{c_s}(\cdot)$, with $p_{c_s} = g_{c_s}(v_s)$. Also, we assume no "cannibalization" effect. As a result, the losses resulting from the interferences between the various turbines are negligibly small. We further assume that all turbines are constructed on towers of equal height and that all the turbines are experiencing the same wind speed. Under such assumptions, the total output of the wind farm is obtained by scaling the output of the individual turbines:

$$p_s = g_s(v_s) = \sum_{c_s \in \mathcal{C}_s} n_{c_s}.p_{c_s} = \sum_{c_s \in \mathcal{C}_s} n_{c_s}.g_{c_s}(v_s). \quad (1)$$

Now, as the wind speed is random, the wind power output is also random and is represented by an *r.v.* $\underset{\sim}{P}_s$, corresponding to the wind speed *r.v.* $\underset{\sim}{V}_s$ driving the wind farm turbines. We have: $\underset{\sim}{P}_s = g(\underset{\sim}{V}_s)$. The wind speed $\underset{\sim}{V}_s$ *c.d.f.* [*p.d.f.*] is denoted by $F_{\underset{\sim}{V}_s}(\cdot)[f_{\underset{\sim}{V}_s}(\cdot)]$. We can analytically express the *c.d.f.* and *p.d.f.* of the wind power *r.v.* $\underset{\sim}{P}_s$ [13].

[1]The adoption of an hourly resolution simplifies the notation and makes the understanding of the steps easier. The scheme is sufficiently general, however, to allow the adoption of other resolution levels.

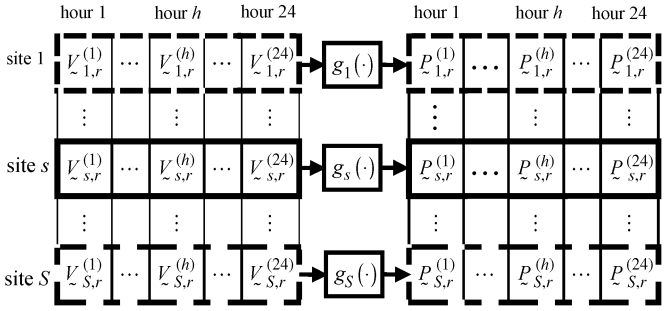

Fig. 2. Representation of the 24 wind power *r.v.*s for regime $\boldsymbol{R}_r$ at the S sites.

We associate with each wind speed regime $\boldsymbol{R}_r$ a collection of $S \cdot H$ *r.v.*s, one for each site and each subperiod of the day. For an hourly resolution of the wind speed data, each of the $S \cdot 24$ wind speed *r.v.s* $\underset{\sim}{V}_{s,r}^{(h)}$ results in a power output $\underset{\sim}{P}_{s,r}^{(h)}$ with: $\underset{\sim}{P}_{s,r}^{(h)} = g_s(\underset{\sim}{V}_{s,r}^{(h)})$, $h = 1, \ldots, 24$, $s = 1, \ldots, S$. We find it convenient to use a matrix representation of the collection of $\underset{\sim}{V}_{s,r}^{(h)}$ and corresponding $\underset{\sim}{P}_{s,r}^{(h)}$ in an array with S rows and 24 columns. We conceptually depict this representation in Fig. 2. For regime $\boldsymbol{R}_r$, we are interested in the total hourly wind power production $\underset{\sim}{P}_{\Sigma,r}^{(h)}$ from the S sites given by

$$\underset{\sim}{P}_{\Sigma,r}^{(h)} = \sum_{s \in \mathcal{S}} \underset{\sim}{P}_{s,r}^{(h)} = \sum_{s \in \mathcal{S}} g_s\left(\underset{\sim}{V}_{s,r}^{(h)}\right). \quad (2)$$

We next approximate the *c.d.f.* of the 24 hourly wind power *r.v.s* $\underset{\sim}{P}_{\Sigma,r}^{(h)}$. This step may be performed making use of numerical approximation techniques for the data samples of each regime. We may reduce the computational burden by introducing additional assumptions. With the wind speed regime-based approach, we have identified the typical patterns of wind speeds which simultaneously occur at the S wind farm locations. In this way, we implicitly capture the correlation between the daily wind speed patterns at the S sites. The sites are assumed to be geographically well removed from one another so that the correlation among any pair of sites is negligibly small. As such, we may assume without loss of generality that the power outputs are independent *r.v.s*. Consequently, the corresponding wind power *r.v.*s are also statistically independent. We construct an estimate of the *p.d.f.* of $\underset{\sim}{P}_{\Sigma,r}^{(h)}$, by iteratively convolving the S *p.d.f.*s of the $\underset{\sim}{P}_{s,r}^{(h)}$.

III. Production Simulation Tool for Systems With Integrated Wind Resources

The probabilistic simulation tool is widely used to evaluate the expected energy produced by each unit in the resource mix over a specified period of time and determine the expected system production costs, the expected emissions, the reliability indices, and other variable effects over the specified study period. The probabilistic simulation is used in longer-term planning studies to investigate issues such as the optimal resource mix determination to serve the forecasted load. We

briefly review probabilistic production simulation to introduce the related notation; more details are available elsewhere [8].

The specification of the production simulation periods is dependent on the planning horizon of the study and the level of detail required. For the realistic emulation of the actual system operations, we define the simulation periods to cover the entire study period and in a way that captures seasonality effects, as well as changes in the resource mix and resource characteristics, the new policy and legislative initiatives, the investment decisions, and the maintenance schedule of the resources. The simulation periods are non-overlapping and may have unequal durations. Each simulation period consists of a number of subperiods that determine the duration. We denote by T_t the number of subperiods in the simulation period t and define $\mathscr{T}_t \triangleq \{1, \ldots, T_t\}$ to be the subperiod index set for the simulation period t. We perform probabilistic simulation over each simulation period.

For each simulation period, the required supply and demand data are collected to run the simulation with the resolution that is commensurate with the level of detail desired for the study. The resolution entails a specification of the smallest indecomposable unit of time and impacts, therefore, the nature of the load and resource representation. The load is assumed to be constant over that time unit and all phenomena of shorter duration cannot be represented in the simulation and are thus ignored. We may view the load as an *r.v.* $\underset{\sim}{L}$ whose probability distribution we estimate from the chronological load data. We refer to the complement of the *c.d.f.* of $\underset{\sim}{L}$ as the inverted load duration curve (*l.d.c.*).

The probabilistic simulation emulates the energy production by each unit in the resource mix used to meet the load in the simulation period t. In our work, we consider a system with the committed set of units committed in period t denoted by $\mathscr{I}_t \triangleq \{i : i = 1, \ldots, I_t\}$. This set is constituted of the units that are not on planned maintenance in period t and which may be scheduled for generation in that period. Each controllable unit has its output level set by the system operator but the output is also a function of the availability of the unit. We model the availability of each unit by a discrete random variable to represent the multi-state capacities with which a unit may be dispatched. In our work, we use a two-state probabilistic representation for the units: either the full unit capacity is available or all the unit is on forced outage. We further assume that the availability *r.v.* of each unit is independent of any other unit and also independent of the load *r.v.*

Each unit may be represented by a single-block or a multiple-block model. Once scheduled, each unit has its blocks loaded in a way to meet the load in the most economic manner. We represent the impacts of the scheduling determined by the unit commitment of the controllable units by a priority list. The list is constructed to reflect the actual economics of the power system operations. Typically, the blocks of the units are loaded in order of increasing prices starting with the cheapest blocks and ending with the most expensive block.

The simulation makes use of the notion of equivalent load *r.v.* Consider the loading of blocks $1, \ldots, j-1$ to meet the load. We compute the equivalent load $\underset{\sim}{L}_{j-1}$ iteratively and each unit is loaded using

$$\underset{\sim}{L}_j = \underset{\sim}{L}_{j-1} + \underset{\sim}{Z}_j \text{ with } \underset{\sim}{L}_0 = \underset{\sim}{L}. \tag{3}$$

In (3), $\underset{\sim}{L}_{j-1}$ is the equivalent load after the first $j-1$ blocks have been loaded and $\underset{\sim}{Z}_j$ is the outage capacity *r.v.* of the jth block to be loaded. We may view $\underset{\sim}{L}_j$ as the uncertain load that is served by the units' blocks loaded after block j is loaded. The computation makes use of the inverted *l.d.c.* $\mathscr{L}(\cdot)$ to successively compute $\mathscr{L}_1(\cdot), \ldots, \mathscr{L}_{j-1}(\cdot)$ as the complements of the *c.d.f.* of the equivalent load *r.v.s* $\underset{\sim}{L}_1, \ldots, \underset{\sim}{L}_{j-1}$. The independence assumption allows the use of convolution for this purpose. The evaluation of the system variable effects makes extensive use of the inverted *l.d.c.*s.

The principal challenge of extending production simulation to systems with integrated wind resources is to mesh the probabilistic framework of production simulation with that for representing the time-dependent variability and intermittency of wind resources. The regime-based wind power output model provides a probabilistic characterization of wind power output over a day. Specifically, the model provides the wind power production *r.v.* for each regime and for each subperiod h of the H subperiods representing the daily period. The incorporation of the diurnal regime-based wind output models into the production simulation framework requires several "synchronization" steps. We describe the "synchronization" using the hourly resolution adopted, but the scheme is sufficiently general to allow the adoption of any desired granularity. Each wind power regime is characterized by a collection of 24 wind power *r.v.s*, one for each hour of the day. To incorporate these models in the production simulation framework, we need the same granularity in the production simulation models.

We consider the load representation in the production simulation and use the hourly resolution for a simulation period t. The hourly random wind output needs to be directly related to the hourly random load that must be met. However, the load *r.v.* $\underset{\sim}{L}$ for the simulation period t provides no temporal information. To "synchronize" the two models, we start with the sample space of the load *r.v.* consisting of the T_t hourly values of load in the simulation period t. We may collect the daily sample values for each day to obtain a subset of 24 hourly load values. In this way, we decompose the sample space into as many subsets J as there are days in the simulation period, with each subset consisting of that day's 24 hourly load values. Conceptually, we may view the sample space as a matrix with J rows and 24 columns. We define for each hour $h = 1, \ldots, 24$ the subsets $\mathscr{T}_t^{(h)}$ of $\mathscr{T}_t$, with each $\mathscr{T}_t^{(h)}$ being the collection of the indices of the hour h of the J days in the simulation period t:

$$\mathscr{T}_t = \bigcup_{h=1}^{24} \mathscr{T}_t^{(h)} \; with \quad \mathscr{T}_t^{(h)} \bigcap_{h \neq h'} \mathscr{T}_t^{(h')} = \varnothing, \quad h \neq h'. \tag{4}$$

We make use of the load samples ℓ_τ, $\tau \in \mathscr{T}_t^{(h)}$ to estimate the *c.d.f.* $F_{\underset{\sim}{L}|h}(\cdot)$ of the *r.v.* $\underset{\sim}{L}$ conditioned on the hour h. The use of the conditional probability allows us to restate the probability of the event that $\underset{\sim}{L} \leq \ell$:

$$\begin{aligned} F_{\underset{\sim}{L}}(\ell) &= Prob\{\underset{\sim}{L} \leq \ell\} = Prob\{\underset{\sim}{L} \leq \ell \; in \; every \; hour \; h\} \\ &= \sum_{h=1}^{24} Prob\{\underset{\sim}{L} \leq \ell | hour \; h\} Prob\{hour \; h\} \\ &= \sum_{h=1}^{24} F_{\underset{\sim}{L}|h}(\ell) \cdot \frac{1}{24} \end{aligned} \tag{5}$$

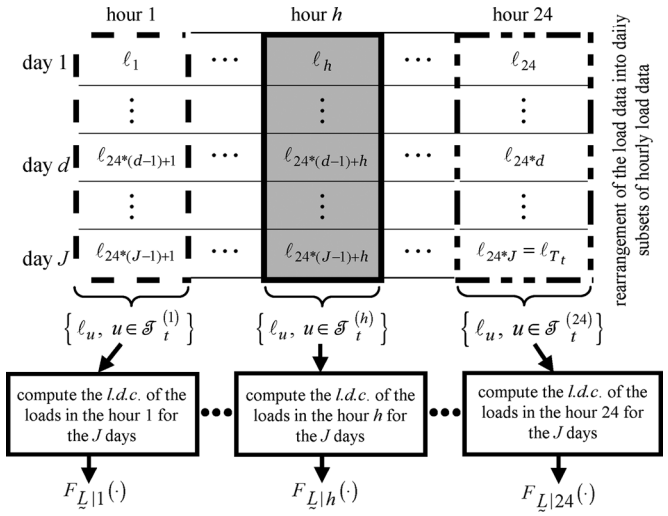

Fig. 3. Process for the load model refinement.

where we make use of the non-overlapping subsets that constitute the sample space and the fact that each such subset has the uniform probability of occurrence of 1/24. In Fig. 3, we depict the classification and its representation for obtaining compatibility with the wind modeling.

The derivation of (5) is easily extended to the conditioning characterization for the equivalent loads $\underset{\sim}{L}_i, i = 1, \ldots, I_t$ since the unit characteristics are uniform for the entire simulation period, i.e., for every hour. We have

$$F_{\underset{\sim}{L}_i}(\ell) = Prob\{\underset{\sim}{L}_i \leq \ell\} = \sum_{h=1}^{24} F_{\underset{\sim}{L}_i|h}(\ell) \cdot \frac{1}{24} \qquad (6)$$

where $F_{\underset{\sim}{L}_i|h}(\cdot)$ denotes the conditional probability of the equivalent load $\underset{\sim}{L}_i$ for hour h. In this way, we can restate all the probabilistic simulation results using the conditional distributions with the conditioning on the hour h of the simulation period.

Thus far, we have discussed the probabilistic simulation with the controllable resources. We next describe the representation of the wind resource impacts by making use of load sample space partitioning in combination with the wind regime dependent output of (2). The uncertain output of each wind turbine is used to supply some of the demand with the remainder being supplied by the controllable units. We construct the uncertain wind output modified load which needs to be served by the controllable units, to which we refer as the "controllable" load $\underset{\sim}{C}$. We directly make use of the hourly decomposition of the load sample space and assume that the load and wind power *r.v.s* are independent for hour h. Consequently, we use the convolution formula to compute the *c.d.f.* of the "controllable" load *r.v.* for each hour which we denote by $F_{\underset{\sim}{C}|h}$. If we consider multiple wind speed regimes, we compute in a similar way the *c.d.f.* $F_{\underset{\sim}{C}|h,r}$ of the controllable load for hour h and wind speed regime $\boldsymbol{R}_r$. In this case, we estimate $F_{\underset{\sim}{C}|r}(\cdot)$ from the 24 $F_{\underset{\sim}{C}|h,r}(\cdot)$ that we compute using an analogous reasoning to the derivation of (5):

$$F_{\underset{\sim}{C}|r}(c) = Prob\left\{\underset{\sim}{C} \leq c | regime\ \boldsymbol{R}_r\right\} = \sum_{h=1}^{24} \frac{1}{24} F_{\underset{\sim}{C}|h,r}(c).$$

For each $F_{\underset{\sim}{C}|r}(\cdot)$, the production simulation for the controllable resources proceeds exactly as in the conventional case but the computation is conditioned on the wind speed regime $\boldsymbol{R}_r$. In this way, we evaluate the figures of merit of the various controllable units by conditioning on the wind speed regime. The value of each metric for a simulation period t is obtained as the probability weighted average of the expected values conditioned on the wind speed regimes.

In our simulation work, we explicitly represent the required reserve levels increase for the accommodation of the fluctuations in the wind resource output by modifying the priority list. Such modifications may entail the loading of additional controllable units and so of the loading order so as to ensure that the required reserves level is met. The paper is focused on the simulation approach for longer-term periods and the unit commitment issues are treated as an exogenously specified input into the simulation. The proposed approach is, indeed, very helpful in answering a broad range of *what if* cases related to the unit commitment issues. Techniques to evaluate the operating reserve requirements of generating systems with renewable energy resources have been proposed in the literature [14]. The required increases in reserves levels, typically, result in an increase in the system production costs and may be viewed as the additional operational costs in the integration of wind resources. We ran multiple sensitivity studies to assess the impacts over a range of increases in the reserves levels.

IV. Simulation Results

We have carried out an extensive set of simulations to demonstrate the capabilities of the proposed tool to capture and quantify the effects that are observed with the integration of wind resources over a wide range of conditions. We devote this section to discuss the testing work and to provide representative results.

We present the simulation results using the so-called *Eastern Test System* (*ETS*) which is based in the PJM region. The *ETS* load is a scaled-down version of the load shape of the PJM system with a 2850 MW peak. We use the 2006 PJM load data with a 144 640 MW peak and the scaling factor of 2850/144 640 to construct the test system load data. In addition, we construct a second synthetic system—the *Midwestern Test System* (*MTS*)—in a similar way based in the MISO region and whose load data is a scaled-down version of the 2006 MISO load data. On the supply side, the *ETS* and *MTS* have sets of controllable units—each consists of 29 units of 8 different technologies. Each supply system represents a slightly modified version of the *IEEE Reliability Test System* (*RTS*) [15]. We use the *RTS* data for the forced outage rates, the number of blocks of the units, and the block capacities. However, each peaking unit is modeled as single block unit and the capacities of some blocks are slightly modified. The unit economics are specified in terms of the heat rate at minimum capacity and the incremental heat rate for each additional block of the unit. For the numerical results discussed here, we use 6 $/MMbtu for the fuel costs. The CO_2 emission rates are identical as those in the *RTS* and are expressed in tons/MWh. In the simulations, we also explicitly represent the scheduled maintenance of the controllable units, which is set up to conform with the requirements specified for the *RTS*. For the wind resources, we consider wind farms located at sites within the PJM and MISO footprints and we make use of the 2006 historical hourly wind speed data at the sites where the wind resources are located

TABLE I
ETS PRODUCTION SIMULATION REFERENCE CASE RESULTS

metric	simulation period	
	week of Jan 2-8, 2006	entire 2006 year
LOLP	$7.78\ 10^{-6}$	$1.26\ 10^{-4}$
EUE (*MWh*)	$2.25\ 10^{-2}$	18.6
expected production costs (*$*)	$1.64\ 10^{7}$	$8.42\ 10^{8}$
expected CO_2 emissions (*lb.*)	$3.93\ 10^{8}$	$2.09\ 10^{10}$

TABLE II
ETS PRODUCTION SIMULATION RESULTS WITH THE INTEGRATION OF A 300 MW WIND FARM AT ALLEGHENY RIDGE, PA

metric	simulation period	
	week of Jan 2-8, 2006	entire 2006 year
LOLP	$3.46\ 10^{-6}$	$5.26\ 10^{-5}$
EUE (*MWh*)	$1.00\ 10^{-2}$	9.23
expected production costs (*$*)	$1.56\ 10^{7}$	$7.95\ 10^{8}$
expected CO_2 emissions (*lb.*)	$3.88\ 10^{8}$	$2.05\ 10^{10}$

[16]. We run production simulations on the *ETS* and the *MTS* systems with the integrated wind farms. We next discuss a set of representative results taken from the extensive production simulation studies we performed.

We start out by the specification of the reference case for the test system simulation consisting of simply the controllable resource mix. We evaluate the variable effects without any wind generation. For discussion purposes, we arbitrarily select the one-week simulation period corresponding to the week of January 2–8, 2006. The values of the Loss of Load Probability (*LOLP*), expected unserved energy (*EUE*), expected production costs, and CO_2 emissions computed for this week and for the entire 52-week period are presented in Table I.

We examine the impacts of the wind resource integration on the system variable effects. For the study, we consider a 200-turbine wind farm using GE 1.5 xle turbines and sited at Allegheny Ridge, PA. Each unit has a 1.5 MW rated power output with the following wind speed parameters: $v_i = 3\ \mathrm{m/s}$, $v_o = 20\ \mathrm{m/s}$, $v_r = 12\,\mathrm{m/s}$. This 300 MW nameplate capacity wind farm represents a 5.6% wind penetration for the *ETS*. Note that the wind penetration is defined as the fraction of the total energy demand served by wind resource generation. We use a single-regime wind speed representation to determine the "controllable" load. The production simulation results are summarized in Table II. Clearly, the integration of the wind farm increases markedly the system reliability since both the *LOLP* and the *EUE* indices are reduced by more than a factor of 2. In addition, the displacement by the wind generators of the polluting fossil units reduces the system production costs and lowers emissions by a few percent.

We next investigate the impacts of the wind resource installation magnitude on the variable effects of the *ETS* system with integrated wind resources by considering a wind farm located in Allegheny Ridge, PA, with nameplate capacity of 300 MW, 600 MW, and 900 MW. We compare the variable effects computed using a single regime wind representation for the three different wind farm sizes and report in Table III the changes in the metrics with respect to those for the base case. We remark that the expected production costs and CO_2 emissions decrease linearly with the size of the wind farm. Indeed, for the considered wind penetrations, every additional MW of wind generation displaces the more expensive units whose economic characteristics have the same order of magnitude.

TABLE III
VALUES OF METRICS FOR THE WIND FARM INTEGRATION INTO THE MIDWESTERN TEST SYSTEM AT DIFFERENT PENETRATIONS

changes in the figure of merit (%)	nameplate capacity (*MW*) – penetration (% of total energy demanded)		
	300 – 5.6	600 – 11.2	900 – 16.8
LOLP reduction	52.3	63.5	69.5
EUE reduction	52.0	63.4	69.4
production costs reduction	5.4	9.6	13.8
CO_2 emission reduction	1.8	3.7	6.0

We observe the diminishing returns in reliability improvements with the deeper penetration of wind resources. Such nonlinear behavior is rather pronounced. We study further this behavior by evaluating the effective load carrying capability—*ELCC* [17]—of the wind farm. This metric provides a meaningful measure of the effective load served by the capacity addition of a new resource, i.e., the *ELCC* determines the load increment that a system can support with the modified resource mix, at the same reliability level. The application of *ELCC* to the determination of capacity credits is presented in [18]. We use the *ELCC* as an effective capacity value for a wind resource since it captures the reliability benefits resulting from its integration into the system. We evaluate the *ELCC* of the 300 MW wind farm by comparing the *LOLP* of the *ETS* with and without the wind farm for different peak loads and conclude that the 300 MW wind farm has a 103 MW *ELCC*.

Clearly, the *ELCC* is a function of the wind penetration. In Fig. 4, we provide a plot of the *ELCC* as a function of the size of the wind farm for the *ETS*. The *ELCC* plot reinforces the notion that the integration of a wind farm into a system with a low wind penetration is far more beneficial in reliability terms than with a higher penetration. Such behavior arises due to the intermittency effects of wind: for any penetration level, there is a fraction of time in the simulation period with no wind power generation and so with no contribution to meeting system demand and, consequently, no contribution to improving the system reliability metrics from additional capacity at the same location.

The regime-based wind speed representation implicitly takes into account the seasonality of the wind power production. We illustrate this important feature of the simulation approach by considering a 300 MW wind farm located in Allegheny Ridge integrated into the *ETS*. For a three-regime representation of the wind speed, we perform the simulation using weekly periods. For each week of 2006, we determine the distribution functions of the "controllable" load conditioned on the three wind speed

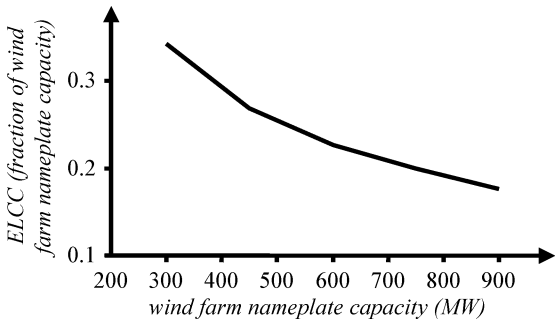

Fig. 4. Effective load carrying capability of a wind farm with different nameplate capacity values.

TABLE IV
QUARTERLY PROBABILITY DATA FOR THE THREE WIND SPEED REGIMES

quarter	regime		
	R_1	R_2	R_3
Q_1	0.20	0.44	0.36
Q_2	0.56	0.42	0.02
Q_3	0.54	0.45	0.01
Q_4	0.21	0.55	0.24

TABLE V
ETS PRODUCTION SIMULATION RESULTS FOR Q_1

metric	regime (probability)			Q_1 weighted average
	R_1 (0.20)	R_2 (0.44)	R_3 (0.36)	
LOLP	$1.07\ 10^{-5}$	$5.77\ 10^{-6}$	$1.77\ 10^{-6}$	$1.3\ 10^{-6}$
EUE (*MWh*)	0.40	0.22	0.067	0.20
expected production costs ($)	$2.07\ 10^{8}$	$1.99\ 10^{8}$	$1.86\ 10^{8}$	$1.95\ 10^{8}$
expected CO_2 emissions (*lb.*)	$4.95\ 10^{9}$	$4.86\ 10^{9}$	$4.70\ 10^{9}$	$4.82\ 10^{9}$

regimes. We partition the 52 weeks of the year 2006 into four quarters Q_i, $i = 1, 2, 3, 4$, each consisting of 13 weeks and display the quarterly data for the three wind-speed regimes using the weights determined by the clustering algorithm shown in Table IV. The variable effects for Q_1 under each of the three regimes and the weighted average are shown in Table V. The values for $Q_2 - Q_4$ and for the whole year are shown in Table VI. We note the strong dependence of the production simulation results on the wind regime. For instance, the *LOLP* computed when considering the regime R_1 is nearly 6 times larger than that obtained for regime R_3. Similarly, the expected production costs and CO_2 emissions are, respectively, 11% and 5% higher, so the results clearly illustrate the dependence of the economics and reliability impacts on the daily wind speed patterns.

The seasonality is also important in observing the pronounced differences between the values of the reliability metrics for the four quarters in 2006. For instance, the *LOLP* is approximately

TABLE VI
ETS VARIABLE EFFECTS OF THE FOR $Q_2 - Q_4$ AND THE ENTIRE YEAR

metric	quarter			entire 2006 year
	Q_2	Q_3	Q_4	
LOLP	$1.74\ 10^{-5}$	$2.63\ 10^{-4}$	$3.81\ 10^{-6}$	$7.13\ 10^{-5}$
EUE (*MWh*)	0.64	9.70	0.14	10.68
expected production costs (10^8 $)	1.90	2.22	1.87	7.94
expected CO_2 emissions (10^9 *lb.*)	5.19	5.64	4.87	2.05

TABLE VII
IMPACT OF THE DIVERSIFICATION OF THE WIND FARM LOCATIONS ON THE *MTS* RELIABILITY

metric	300 *MW* wind farm in Camp Grove, IL	four 66 *MW* wind farms at the Midwestern locations
LOLP	$7.92\ 10^{-5}$	$6.57\ 10^{-5}$
EUE (*MWh*)	11.7	9.67

200 times larger during Q_3 than during Q_1, so the vast majority of the loss of load events occur during Q_3 that includes the summer months with typically the highest loads of the year. There are similar findings for the *EUE*. The results in Table VI also indicate the corresponding pronounced impacts on the expected production cost cases. The portfolio effect of wind farms at multiple sites results in a smoother wind power production with less variability and less pronounced intermittency effect.

Indeed, the location diversity improves the system reliability. For the case study, we start with the evaluation of the reliability metrics for the *MTS* with a 300 MW wind farm integrated at Camp Grove, IL, and compare its metrics with those. We also run production simulations in the case where the *MTS* wind resources are constituted of four 66 MW wind farms—composed of 44 GE turbines each—located at the four Midwestern sites: Camp Grove, IL, Fenton, MN, Langdon, ND, and Harvest, MI. The number of turbines was determined so that the expected wind energy production over the year 2006 is the same as that of the 300 MW wind farm sited in Camp Grove. In Table VII, we compare the *LOLP* and the *EUE* computed for these two cases. We remark that the reliability metrics have been significantly reduced by the dispersion of the wind farm locations.

The illustrations provided in this section demonstrate the effectiveness of the proposed approach to quantify the economic, environmental, and reliability benefits obtained with the integration of wind resources into the grid.

V. CONCLUSION

In this paper, we present the development and testing of a simulation approach for evaluating the variable effects of power systems with integrated wind resources over longer-term periods. The ability to quantify the impacts of wind resources on the economics of electricity supply, the emission outputs, and the system reliability makes the approach very effective in planning evaluations, investment decisions, regulatory filings, and

policy analysis. Our illustrative examples demonstrate the capability of the proposed approach to answer a broad range of *what-if* questions for realistic-sized power systems. We present results selected from the extensive simulation studies to quantify the impacts of wind resources on the system variable effects for different levels of penetration and also with location diversity. Our investigations provide useful insights into the contributions of wind resources in the efficient utilization of controllable generation resources and reliability and environmental effects. The extension of the probabilistic simulation approach to incorporate the variable and intermittent outputs of wind resources constitutes a major improvement in the capability to emulate systems with integrated resources that have time-varying and intermittent generation characteristics.

The proposed approach provides a good starting point for the development of additional simulation capabilities to study systems with other renewable resources, such as solar technology applications, utility-scale storage devices, and time-varying demand-side activities, such as demand response resources. Indeed, the regimes-based approach described in the paper is an effective methodology for capturing both the seasonal and the diurnal variability of time-dependent resources. We are currently developing a comprehensive approach which can effectively emulate the operation of a system with demand-side, renewable, storage, and other time-dependent resources. Our efforts will be described in future publications.

REFERENCES

[1] DSIRE—Database of State Incentives for Renewables & Efficiency. [Online]. Available: http://www.dsireusa.org/.

[2] "2010: Offshore and Eastern Europe New Growth Drivers for Wind Power in Europe". [Online]. Available: http://ewea.org/fileadmin/ewea_documents/documents/statistics/EWEA_Annual_Statistics_2010.pdf.

[3] "ERCOT Operations Report on the EECP Event of February 26, 2008", 2008. [Online]. Available: http://www.ercot.com/content/meetings/ros/keydocs/2008/0313/07._ERCOT_OPERATIONS_REPORT_EECP022608_public.doc.

[4] E. Ela and B. Kirby, "ERCOT Event on February 26, 2008: Lessons Learned", NREL, CO, Tech. Rep. NREL/TP-500-43373, Jul 2008. [Online]. Available: http://www.nrel.gov/wind/systemsintegration/pdfs/2008/ela_ercot_event.pdf.

[5] R. Doherty and M. O'Malley, "A new approach to quantify reserve demand in systems with significant installed wind capacity," *IEEE Trans. Power Syst.*, vol. 20, no. 2, pp. 587–595, May 2005.

[6] J. C. Smith, M. R. Milligan, E. A. DeMeo, and B. Parsons, "Utility wind integration and operating impact state of the art," *IEEE Trans. Power Syst.*, vol. 22, no. 3, pp. 900–908, Aug. 2007.

[7] H. Gil and G. Joos, "Generalized estimation of average displaced emissions by wind generation," *IEEE Trans. Power Syst.*, vol. 22, no. 3, pp. 1044–1050, Aug. 2007.

[8] A. Wood and B. Wollenberg, *Power Generation, Operation and Control*. New York: Wiley, 1996.

[9] L. Söder and J. Bubenko, Sr., "Capacity credit and energy value of wind power in hydro-thermal power system," in *Proc. 9th Power System Computation Conf.*, Lisbon, Portugal, 1987, pp. 222–225.

[10] V. M. Gomez-Munoz and M. A. Porta-Gandara, "Local wind patterns for modeling renewable energy systems by means of cluster analysis techniques," *Renew. Energy*, vol. 25, no. 2, pp. 171–182, 2002.

[11] G. Gan, C. Ma, and J. Wu, *Data Clustering: Theory, Algorithms, and Applications*. Philadelphia, PA: SIAM, 2007.

[12] G. Masters, *Renewable and Efficient Electric Power Systems*. New York: Wiley, 2007.

[13] S. H. Karaki, R. B. Chedid, and R. Ramadan, "Probabilistic performance assessment of wind energy conversion systems," *IEEE Trans. Energy Convers.*, vol. 14, no. 2, pp. 217–224, Jun. 1999.

[14] A. M. Leite da Silva, W. S. Sales, L. A. F. Manso, and R. Billinton, "Long-term probabilistic evaluation of operating reserve requirements with renewable sources," *IEEE Trans. Power Syst.*, vol. 25, no. 1, pp. 106–116, Feb. 2010.

[15] C. Grigg *et al.*, "The IEEE reliability test system-1996. A report prepared by the reliability test system task force of the application of probability methods subcommittee," *IEEE Trans. Power Syst.*, vol. 14, no. 3, pp. 1010–1020, Aug. 1999.

[16] Eastern Wind Integration and Transmission Study—NREL Data. [Online]. Available: http://wind.nrel.gov/public/EWITS/.

[17] L. L. Garver, "Effective load carrying capability of generating units," *IEEE Trans. Power App. Syst.*, vol. PAS-85, no. 8, pp. 910–919, Aug. 1966.

[18] M. Amelin, "Comparison of capacity credit calculation methods for conventional power plants and wind power," *IEEE Trans. Power Syst.*, vol. 24, no. 2, pp. 685–691, May 2009.

Nicolas Maisonneuve received his B.S. degree in Electrical and Computer Engineering from Supelec, Paris, France in 2007 and his M.S. degree in Electrical and Computer Engineering at the University of Illinois at Urbana-Champaign as well as his M.S. degree in Electrical and Computer Engineering from Supelec in 2009. His research interests include power system operations and planning, electricity markets and renewable energy.

George Gross (F'88) is Professor of Electrical and Computer Engineering and Professor, Institute of Government and Public Affairs, at the University of Illinois at Urbana-Champaign. His current research and teaching activities are in the areas of power system analysis, planning, economics and operations and utility regulatory policy and industry restructuring. In the 1999–2000 academic year, he was a Visiting Professor at a number of Italian institutions including University of Pavia, Politecnico di Milano and Politecnico di Torino.

His undergraduate work was completed at McGill University, and he earned his graduate degrees from the University of California, Berkeley. He was previously employed by Pacific Gas and Electric Company in various technical, policy and management positions. Dr. Gross won the Franz Edelman Management Science Achievement Award in 1985 and is the recipient of several prize paper awards. He has consulted widely to organizations in North and South America, Europe and Asia.